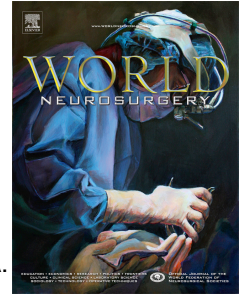


# Accepted Manuscript



Biomechanical and endplate effects on nutrient transport in the intervertebral disc

Morgan B. Giers, PhD, Bryce T. Munter, MS, Kyle J. Eyster, MS, George D. Ide, MD, Anna G.U.S. Newcomb, MS, Jennifer N. Lehrman, MS, Evgenii Belykh, MD, Vadim A. Byvaltsev, MD PhD, Brian P. Kelly, PhD, Mark C. Preul, MD, Nicholas Theodore, MD

PII: S1878-8750(16)31353-5

DOI: [10.1016/j.wneu.2016.12.041](https://doi.org/10.1016/j.wneu.2016.12.041)

Reference: WNEU 5002

To appear in: *World Neurosurgery*

Received Date: 10 November 2016

Revised Date: 9 December 2016

Accepted Date: 10 December 2016

Please cite this article as: Giers MB, Munter BT, Eyster KJ, Ide GD, Newcomb AGUS, Lehrman JN, Belykh E, Byvaltsev VA, Kelly BP, Preul MC, Theodore N, Biomechanical and endplate effects on nutrient transport in the intervertebral disc, *World Neurosurgery* (2017), doi: 10.1016/j.wneu.2016.12.041.

This is a PDF file of an unedited manuscript that has been accepted for publication. As a service to our customers we are providing this early version of the manuscript. The manuscript will undergo copyediting, typesetting, and review of the resulting proof before it is published in its final form. Please note that during the production process errors may be discovered which could affect the content, and all legal disclaimers that apply to the journal pertain.

**Biomechanical and endplate effects on nutrient transport in the intervertebral disc**

Morgan B. Giers, PhD<sup>1</sup>

Bryce T. Munter, MS<sup>2</sup>

Kyle J. Eyster, MS<sup>2</sup>

George D. Ide, MD<sup>1</sup>

Anna G. U. S. Newcomb, MS<sup>1,2</sup>

Jennifer N. Lehrman, MS<sup>1</sup>

Evgenii Belykh, MD<sup>1</sup>

Vadim A. Byvaltsev, MD PhD<sup>3</sup>

Brian P. Kelly, PhD<sup>1</sup>

Mark C. Preul, MD<sup>1</sup>

Nicholas Theodore, MD<sup>1</sup>

<sup>1</sup>Department of Neurosurgery

Barrow Neurological Institute

St. Joseph's Hospital and Medical Center

Phoenix, Arizona

<sup>2</sup>School of Biological and Health Systems Engineering

Arizona State University

Tempe, Arizona

<sup>3</sup>Irkutsk Scientific Center of Surgery and Traumatology

Irkutsk, Russia

**Correspondance:** Nicholas Theodore, MD

c/o Neuroscience Publications; Barrow Neurological Institute

St. Joseph's Hospital and Medical Center

350 W. Thomas Rd.; Phoenix, AZ 85013

Tel: 602.406.3593; Fax: 602.406.4104

E-mail: Neuropub@dignityhealth.org

**DISCLOSURES:** None

**FINANCIAL SUPPORT:** This work was supported by the Beverly and Millard Seldin Family, and the Russian Science Foundation (Project No. 15-15-30037) and, in part, by Newsome Endowment in Neurosurgery Research funds to Dr. Preul.

**ACKNOWLEDGMENTS:** The authors thank the Beverly and Millard Seldin Family, and the Russian Science Foundation (Project No. 15-15-30037) for their support.

**SUBMISSION CATEGORY:** Original Article

**ABSTRACT**

**Background:** Physical data are lacking on nutrient transport in human intervertebral discs (IVDs), which supports regeneration. Our objective was to study nutrient transport in porcine IVDs to determine the effects of biomechanical and physiological factors.

**Methods:** In vitro testing of whole porcine IVDs was performed under different loading conditions. Fifty cervical, thoracic, and lumbar discs with attached end plates were removed from 4 Yorkshire pigs (90-150 pounds). Discs were placed in Safranin O or Fast Green FCF histological stains in diffusion or diurnal compression-tested groups. The end plate was studied by using polyurethane to block it. Traction was studied with a mechanical testing frame. Discs were cut transversely and photographed. Images were analyzed for depth of annulus fibrosus (AF) stained. The nucleus pulposus (NP) was assigned a staining score.

**Results:** Results showed no difference in AF staining between the two stains ( $P=0.60$ ). The depth of AF staining did not increase ( $P=0.60$ ) due to convection or disc height change via diurnal loading. The NP in all open end plate samples was completely stained by day 3. NP staining was decreased in blocked end plate samples ( $P=0.07$ ) and AF staining was significantly less in traction samples than in diffusion-only samples ( $P=0.04$ ).

**Conclusions:** This method showed that most small molecule nutrient transport occurs via the end plate. Compressive load was a negligible benefit or hindrance to transport. Traction hindered transport in the short term. This method can be used to study strategies for increasing nutrient transport in IVDs.

**RUNNING TITLE:** Biomechanical effects on IVD nutrition

**KEYWORDS:** Annulus fibrosus; biomechanics; calcification; cell function; extracellular matrix; intervertebral disc; nucleus pulposus; nutrient transport; regeneration; spine

**ABBREVIATIONS:**

AF, annulus fibrosus

ANOVA, analysis of variance

FG, Fast Green FCF stain

IVD, intervertebral disc

NP, nucleus pulposus

SO, Safranin O stain

**HIGHLIGHTS**

- The low-nutrient-transport structure of human IVD is a major barrier to regeneration.
- Most small molecule transport in IVDs occurs via the end plate.
- Disc compression does not increase or decrease nutrient transport in IVDs.
- Traction decreases nutrient transport in the short term.
- Stain baths enable study of biomechanical effects on nutrient transport in IVDs.

## INTRODUCTION

Degeneration of the intervertebral disc (IVD) is the leading cause of back pain. More than 85% adults over 50 years of age show evidence of disc degeneration.<sup>1</sup> As people age, structural changes occur in the disc extracellular matrix, resulting in calcification of the disc end plate. The IVD is the largest avascular structure in the human body, so changes in disc structure and subsequent small changes in nutrient supply can threaten the survival of IVD cells. As cells die, the ability of the disc to remodel its extracellular matrix declines and the disc degenerates. Degenerative disc disease causes pain in multiple ways, such as through the ingrowth of nerves in the IVD, facet joint arthritis from disc thinning, and disc bulging that puts pressure on nearby nerve roots. Furthermore, degenerative disc disease is often a precursor to osteoarthritis of the spine, spinal stenosis, and pain that decreases the quality of life of patients.

Common treatments for degenerative disc disease focus on symptom management rather than IVD treatment. When conservative treatments fail, then surgery is recommended. Spinal fusion is the most common surgical treatment, yet it has poor long-term success rates in pain relief and can cause wear on adjacent segments.<sup>2</sup> Artificial disc replacements, such as the SB Charité (DePuy Spine, Raynham, MA), showed evidence of frequent complications as early as ten years after implantation and provided mixed long-term outcomes.<sup>3, 4</sup> There are currently no successful treatments specifically targeting degenerative IVDs.

The IVD can be subdivided into four segments: 1) the annulus fibrosis (AF), 2) the nucleus pulposus (NP), 3) the cartilaginous end plates, and 4) the bony end plates. The stiff AF is composed of approximately 15-25 layers of collagen fiber lamellae arranged in concentric circles around the soft gelatinous NP.<sup>5</sup> The cartilaginous end plates are thin layers of hyaline cartilage that act as a barrier between the NP and the cancellous bone above it and below it.<sup>6</sup> The end

plates are the primary means of contact between the disc and the vascular supply: small capillaries penetrate the cartilaginous end plates and bone marrow cavities contact their periphery.<sup>6</sup> During aging, the decrease in capillary frequency and calcification of the marrow cavities and cartilaginous end plates is thought to be the primary reason for a decrease in nutrient supply to both the AF and the NP.

A major barrier to IVD regeneration is the lack of an environment conducive to cell survival in this low-nutrient-transport structure. The cells of the IVD are constantly building and destroying the extracellular matrix of the IVD as a way to repair proteins damaged as part of normal biological activity. As cells die of starvation, the balance is shifted and the extracellular matrix begins to degrade, ultimately resulting in a loss of IVD tissue. Nutrient transport in a healthy IVD is thought to occur primarily through the end plate, with glucose entering the IVD via diffusion. However, physical data on this course of action are scarce, particularly for whole IVDs. Most of the knowledge about nutrient transport in the disc emanates from mathematical modeling, and such models, along with the few existing *in vivo* experiments, often report conflicting results. For instance, Malandrino et al.<sup>7</sup> reported that mechanical loading increases nutrient transport by decreasing the disc height, whereas Jackson et al.<sup>8,9</sup> reported that mechanical loading decreases nutrient transport by decreasing the diffusion coefficient through the extracellular matrix. Additionally, Gullbrand et al.<sup>10</sup> reported that the nutrient transport can be both increased or decreased depending on the magnitude of the load in rabbit models.

In this *in vitro* study, we investigated nutrient transport in the porcine IVD to determine the effects of biomechanical and physiological factors on it. The end plates of the discs were either blocked or unblocked to simulate calcification of the cartilaginous end plate in humans.



Furthermore, external manipulations were explored to determine whether they could increase nutrient transport in the disc.

## **MATERIAL AND METHODS**

### **Disc Harvest and Specimen Preparation**

Whole spines were donated from another laboratory within 24 hours of euthanasia. Spines used in the study were from 4 Yorkshire pigs of both sexes that weighed 90 to 150 pounds and were ages 3 to 4 months at the time of euthanasia. A reciprocating bone saw was used to remove 50 whole intervertebral cervical, thoracic, and lumbar discs with end plates attached from all but one spine, which was kept intact. The end plates were scrubbed under running water with a wire brush to remove blood clots. Discs were divided into containers of 3 discs, each containing equally spaced segments from the low, medium, and high levels of the spine. The discs were shaved using an air-driven surgical drill and a round bur to make them of equal height. No more than 2 mm of bone was left attached to the cartilaginous end plate. Disc segments were cryofrozen according to the method described by Lam et al., which showed that cryofreezing had no effect on the biomechanical properties of the disc.<sup>11</sup> Briefly, disc segments were cryofrozen in a 100 mL/disc solution of 10% propylene glycol, 10% dimethyl sulfoxide, and 80% Dulbecco's Modified Eagle Medium. The discs were incubated for 2 hours at 4°C, then slowly cooled to -80°C by placing the containers into a 1.5-inch Styrofoam box. The whole spine was dampened by 1× phosphate-buffered saline and frozen at -80°C.

The whole spine was used for traction testing and specimens were prepared differently for the compression and diffusion samples. The spine was defrosted and cut into segments that included an IVD with whole vertebral bodies on either side. Every other IVD was sacrificed to

maintain a full vertebral body. The vertebral bodies were left attached in these samples because more surface area was required to mount the specimen for the traction test; however, the vertebral bodies on either side of the IVD were resected through the end plate using an air-driven surgical drill with a round burr to allow similar stain access to the end plate. The entire vertebra was hollowed out, leaving no more than 2 mm of bone attached to the cartilaginous end plate. Furthermore, the facets were removed using the drill and rongeurs to allow unrestricted motion of the disc.

### **Stain Preparation**

Two different histological stain preparations were used, Safranin O (SO) and Fast Green FCF (FG). SO stains proteoglycans, whereas FG is a non-specific non-collagenous protein stain. Both stains were prepared at 2.85 mM in 1× phosphate-buffered saline.

### **Diffusion Testing**

Discs tested with diffusion only were placed in 200 mL/disc baths of histological stains SO or FG. Diffusion discs were agitated for 1, 3, 5, or 7 days (n=3). Disc containers were chosen at random, with randomization performed via Microsoft Excel (Microsoft Corp., Redmond, WA).

### **Compression Testing**

Loaded discs were also placed in a stain bath, as described above in the Stain Preparation subsection, and placed under a static 50 lb/disc load for  $16.1 \pm 0.15$  hours. The load was then removed for  $7.8 \pm 0.25$  hours to replicate the diurnal cycle normally experienced by humans.

Each disc was sandwiched between 2 commercially available squares of metal screen (1 3/4×1 3/4 inches). A perforated cylinder (for a 1 1/2-inch sink drain) was placed on top of each disc to ensure adequate stain flow over the end plates (Figure 1). The discs were placed an even distance apart in a 22 L bucket and covered with 1.75 L of SO. A second bucket (8.5 L) was placed on top of the drain covers, and weights were stacked inside the smaller bucket to distribute a load on the discs.

In 3 compressed discs, polyurethane (Rust-Oleum, Vernon Hills, IL) was used to block the end plate to determine the importance of the end plate. The end plates of blocked discs were painted with 1 thick layer of polyurethane.

### **Traction Testing**

Data on nutrient transport in IVDs under traction was obtained by attaching the caudal and rostral ends of each motion segment (posterior elements removed) to blocks of fast-curing resin (Smooth-Cast 300Q, Smooth-On, Inc., Easton, PA) using small bone screws and customized fixtures (Figure 2, left). The fixtures allowed fluid to enter the hollow center of the vertebral body and come into contact with the end plate. Each potted specimen was mounted in a standard servohydraulic test system (MTS Systems Corp., Eden Prairie, MN) (Figure 2, right). A tensile load was applied via a hook located approximately in line with the vertical neutral axis of the motion segment. The load was applied from a neutral resting position to 223 N (tension) and held constant for 16 hours, then unloaded to 5 N (tension) for 8 hours. Testing was performed with discs in an SO solution.

### Stain Evaluation

After staining, the discs were rinsed under running tap water, soaked in tap water for 10 minutes, and cut in half through the transverse plane. These steps were taken to avoid dye on the exterior of the disc being transferred into the disc by the scalpel blade. Images with 72 dpi resolution or greater were collected with a digital camera. A ruler was placed in the image for scale. Images were analyzed in ImageJ image processing software (<https://imagej.nih.gov/ij/>) for area of disc stained. The area of the NP, the outer edge of the AF, and the inner edge of the stained region in the AF were measured using the freehand selection tool. Each measurement was performed four times and averaged. Since nutrient transport is reliant on distance regardless of the size of the IVD, the segmented areas were transformed into approximate depth penetrated into the annulus fibrosis (AF) by assuming a circular shape for the disc in the transverse plane, as shown in the following equation.

$$\bar{R} = \sqrt{\frac{A_{Disc}}{\pi}} - \sqrt{\frac{A_{Unstained}}{\pi}}$$

where  $\bar{R}$  is the average radial distance traveled by the stain in the AF,  $A_{Disc}$  is the cross-sectional area of the disc, and  $A_{Unstained}$  is the area of unstained AF. The NP was assigned a score of 1 (no staining), 2 (some staining), or 3 (full staining).

### Statistical Analysis

Statistica software (StatSoft, Inc., Tulsa, OK) was used to perform all statistical analysis. For the data on stain penetration in the AF over time, a repeated measures analysis of variance (ANOVA) was performed. A one-way ANOVA was used to compare stain penetration in the AF for different loading schemes. A two-tailed Student *t* test was used post hoc for all significant

ANOVA data and for comparison of AF staining in blocked and unblocked end plate samples. For the data on NP staining scores over time, the Friedman ANOVA for nonparametric data was used. The Kruskal-Wallis test was used to compare NP staining scores for different loading schemes. The Mann-Whitney U test was used post hoc for all significant ANOVA data and for comparison of AF staining in blocked and unblocked end plate samples.

## RESULTS

In general, the stain penetrated the end plate and traveled quickly throughout the NP, with full staining occurring on days 1-3 (Figure 3). The stain also penetrated radially through the AF quite slowly, taking up to 7 days to fully stain. The depth stain that traveled into the AF was nearly linear over time, as might be expected from diffusion-only transport (Figure 4). There was no difference in the depth of AF stained between the FG stain and the SO stain ( $P=0.60$ ) (Figure 4). There was no significant increase ( $P=0.60$ ) in the depth of staining in the AF due to the addition of convection via diurnal loading. Only 6% (1/16 samples) of the open end plate samples had no NP staining on day 1, and by day 3, the NP in all open samples was completely stained (Figure 5). The blocked end plate samples had decreased NP staining that was not significant ( $P=0.07$ ) (Figure 6A). No significant difference in staining of the AF was found in the blocked end plate samples compared to the open end plate samples ( $P=0.25$ ) (Figure 6B). No significant difference was found between NP staining scores by loading state ( $P=0.13$ ) (Figure 7A); however, the AF showed significantly reduced staining with the addition of traction compared to diffusion-only samples ( $P=0.04$ ) (Figure 7B).

## DISCUSSION

In this experiment, we used 2 stains with different binding characteristics but similar diffusion coefficients ( $D_{\text{SO/water}} = 7.11 \times 10^{-6} \text{ cm}^2/\text{s}$ ,<sup>12</sup>  $D_{\text{FG/water}} = 3.9 \times 10^{-6} \text{ cm}^2/\text{s}$ <sup>13</sup>). If stain binding was limiting the nutrient transport, then the final penetration of the disc would be different between the 2 stains. However, since the 2 stains penetrated the discs similarly, then the molar percentage of bound stain was likely negligible in comparison to the unbound stain in the pore. Glucose also has a diffusion coefficient similar to that of the stains used here ( $D_{\text{Glucose/water}} = 6.7 \times 10^{-6} \text{ cm}^2/\text{s}$ <sup>14</sup>). Therefore, these results for SO and FG staining may be similar to the results for glucose transport; however, even if the dye had been significantly affected by binding, comparing the staining under different loading parameters to that of samples using the same dye is still useful in determining how those parameters effect the samples, such as by generally increasing or decreasing transport.

We found that small molecule transport in the IVD is likely to occur due to diffusion rather than convection. Furthermore, small molecules quickly penetrate the end plate and distribute throughout the NP, but such transport originates from outside the IVD and occurs quite slowly through the AF.

The extent of the role played by compression and convection in the transport of nutrients is unknown. Loading of the IVD causes the discs to lose height, which decreases the distance that nutrients must cross; however, compression also causes the diffusion coefficient to decrease by making pores smaller. Furthermore, loading causes interstitial fluid to flow into and out of the disc, which could lead to nutrient transport via convection. These three mechanisms of disc height change, convection, and diffusion coefficient change all affect transport, but which one is most important is not known. Our results showed that compression overall had no effect on stain

transport. Therefore, we believe that these three mechanisms negated each other in this study. Table 1 summarizes the current literature on this topic.<sup>7, 8, 10, 15-20</sup> The conflicting results, particularly from the in vivo data, seem to indicate that mechanical loading could induce transport changes under certain conditions, particularly in the short term,<sup>10</sup> but this study showed that there was no effect over the course of several days for a static diurnal loading scheme.

It has long been known that end plate blockage by calcification decreases transport.<sup>17, 21</sup> We also found a decrease in NP staining with end plate blockage; however, our results fell short of statistical significance.

Traction therapy has been shown to produce some mild benefits to degenerated IVDs as reported in both basic science and clinical literature. For instance, Kuo et al.<sup>22</sup> showed increased porosity and cell viability in discs that received traction treatment in a bioreactor for 3 days. Furthermore, Choi et al.<sup>23</sup> showed improvement with decompression therapy and traction therapy in the preoperative to postoperative treatment course of patients, as measured by decreases in visual analog scale and Oswestry Disability Index scores, whereas their straight leg raise scores increased; however, level 1 evidence for traction therapy is difficult to obtain in the clinic where blinding is impractical. Our results indicate that traction might actually decrease nutrient transport mechanically, either due to changes in pore size or changes in disc height. This study should not be interpreted as opposition to traction therapy, as there may be other benefits to that therapy (e.g., stimulating cellular activity or reducing disc bulging), which were not captured here, or simply a stretching of the supporting musculature of the spine. However, these data show that short-term increases in nutrient transport are not likely to be the cause of any benefit provided by traction.

This study was limited by its use of porcine tissues rather than human tissues. Porcine spines were a conveniently available large-gauge animal spine, whereas human spines can often be expensive or difficult to obtain. Furthermore, porcine spines could be obtained fresh, within 24 hours, and were of more uniformly healthy quality than human spines. Human cadaver spines often have degenerated discs because they are from older individuals. Such disc degeneration can add more realism to an experiment, but it also adds another variable to further complicate the research. Additionally, pigs are quadrupeds and the biomechanics of porcine spines are not the same as those of humans, which could lead to differences in the endplate; however, porcine spines are close in size to human spines and thus are often used as an IVD model.<sup>24, 25</sup> In future work, this team will repeat several of the tests done here with human discs so that the results can be directly compared to further validate this model. Another limitation of this study was that it was performed *in vitro*. Studying transport phenomena *in vitro* is limited by the lack of blood flow through the vascular beds in the end plates. Furthermore, loading schemes *in vitro* vary widely from the loading that occurs *in vivo*. Also, cellular effects are ignored by this model. Cells make up less than 1% of the volume of disc tissue<sup>26</sup> and the stains used in this study bind extracellularly, which allows stain transport to be largely unaffected by cell activity and integrity. Although approximately 20% of the cell population dies in the freezing process,<sup>27</sup> the mechanical integrity remains unchanged,<sup>11</sup> which makes this model a reasonable way to study the effects of biomechanical manipulation without needing an expensive bioreactor system to maintain cell viability. Although the cell viability is not thought to affect this model, thawed discs were rinsed immediately to minimize the toxic effects of the cryoprotectants.<sup>28</sup> Furthermore, in future studies discs will be rinsed and thawed in phosphate-buffered saline instead of tap water.



This model is an economical way to study many different loading and physiological effects on nutrient transport. This team already has work underway to study the effects of endplate calcification and permeability on nutrient transport in human IVDs under dynamic loading conditions using this model.

## **CONCLUSIONS**

We believe that our results show that most small molecule transport occurs via the end plate. Furthermore, there is negligible benefit or hindrance to nutrient transport with the addition of compressive load, and traction actually hinders transport in the short term. This simple method is one way to study strategies for increasing nutrient transport in the IVD, which is a critical barrier to the development of regenerative therapies.

**REFERENCES**

1. Practice parameters: magnetic resonance imaging in the evaluation of low back syndrome (summary statement). Report of the Quality Standards Subcommittee of the American Academy of Neurology. *Neurology*. Apr 1994;44(4):767-770.
2. Virk SS, Niedermeier S, Yu E, Khan SN. Adjacent segment disease. *Orthopedics*. Aug 2014;37(8):547-555.
3. Ross R, Mirza AH, Norris HE, Khatri M. Survival and clinical outcome of SB Charite' III disc replacement for back pain. *J Bone Joint Surg Br*. Jun 2007;89(6):785-789.
4. Punt IM, Visser VM, van Rhijn LW, Kurtz SM, Antonis J, Schurink GWH, van Ooij A. Complications and reoperations of the SB Charité lumbar disc prosthesis: experience in 75 patients. *Eur Spine J*. 2008;17(1):36-43.
5. Salvatierra JC, Yuan TY, Fernando H, Castillo A, Gu WY, Cheung HS, Huant CY. Difference in energy metabolism of annulus fibrosus and nucleus pulposus cells of the intervertebral disc. *Cell Mol Bioeng*. Jun 1 2011;4(2):302-310.
6. Huang YC, Urban JP, Luk KD. Intervertebral disc regeneration: do nutrients lead the way? *Nat Rev Rheumatol*. Sep 2014;10(9):561-566.
7. Malandrino A, Noailly J, Lacroix D. The effect of sustained compression on oxygen metabolic transport in the intervertebral disc decreases with degenerative changes. *PLoS Comput Biol*. 2011;7(8):e1002112.
8. Jackson AR, Huang CY, Brown MD, Gu WY. 3D finite element analysis of nutrient distributions and cell viability in the intervertebral disc: effects of deformation and degeneration. *J Biomech Eng*. 2011;133(9):4004944.

9. Jackson AR, Yuan TY, Huang CY, Brown MD, Gu WY. Nutrient transport in human annulus fibrosus is affected by compressive strain and anisotropy. *Ann Biomed Eng.* Dec 2012;40(12):2551-2558.
10. Gullbrand SE, Peterson J, Ahlborn J, Mastropolo R, Fricker A, Roberts TT, Abousayed M, Lawrence JP, Glennon JC, Ledet EH. ISSLS Prize Winner: Dynamic Loading-Induced Convective Transport Enhances Intervertebral Disc Nutrition. *Spine (Phila Pa 1976)*. Aug 1 2015;40(15):1158-1164.
11. Lam SK, Chan SC, Leung VY, Lu WW, Cheung KM, Luk KD. The role of cryopreservation in the biomechanical properties of the intervertebral disc. *Eur Cell Mater.* Dec 17 2011;22:393-402.
12. Heli H, Moosavi-Movahedi AA, Jabbari A, Ahmad F. An electrochemical study of safranin O binding to DNA at the surface. *J Solid State Electrochem.* 2006;11(5):593-599.
13. Werts MH, Raimbault V, Texier-Picard R, Poizat R, Francais O, Griscom L, Navarro JR. Quantitative full-colour transmitted light microscopy and dyes for concentration mapping and measurement of diffusion coefficients in microfluidic architectures. *Lab Chip.* Feb 21 2012;12(4):808-820.
14. Ryckeboer E, Vierendeels J, Lee A, Werquin S, Bienstman P, Baets R. Measurement of small molecule diffusion with an optofluidic silicon chip. *Lab Chip.* 2013;13(22):4392-4399.
15. Urban JP, Holm S, Maroudas A, Nachemson A. Nutrition of the intervertebral disc: effect of fluid flow on solute transport. *Clin Orthop Relat Res.* Oct 1982(170):296-302.
16. Ferguson SJ, Ito K, Nolte LP. Fluid flow and convective transport of solutes within the intervertebral disc. *J Biomech.* Feb 2004;37(2):213-221.

17. Soukane DM, Shirazi-Adl A, Urban JP. Computation of coupled diffusion of oxygen, glucose and lactic acid in an intervertebral disc. *J Biomech.* 2007;40(12):2645-2654.
18. Huang CY, Gu WY. Effects of mechanical compression on metabolism and distribution of oxygen and lactate in intervertebral disc. *J Biomech.* 2008;41(6):1184-1196.
19. Arun R, Freeman BJ, Scammell BE, McNally DS, Cox E, Gowland P. 2009 ISSLS Prize Winner: What influence does sustained mechanical load have on diffusion in the human intervertebral disc?: an in vivo study using serial postcontrast magnetic resonance imaging. *Spine (Phila Pa 1976).* 2009;34(21):2324-2337.
20. Zhu Q, Jackson AR, Gu WY. Cell viability in intervertebral disc under various nutritional and dynamic loading conditions: 3D finite element analysis. *J Biomech.* 2012;45(16):2769-2777.
21. Mokhbi Soukane D, Shirazi-Adl A, Urban JPG. Investigation of solute concentrations in a 3D model of intervertebral disc. *Eur Spine J.* 2009;18(2):254-262.
22. Kuo YW, Hsu YC, Chuang IT, Chao PH, Wang JL. Spinal traction promotes molecular transportation in a simulated degenerative intervertebral disc model. *Spine (Phila Pa 1976).* Apr 20 2014;39(9):E550-556.
23. Choi J, Lee S, Hwangbo G. Influences of spinal decompression therapy and general traction therapy on the pain, disability, and straight leg raising of patients with intervertebral disc herniation. *J PhysTher Sci.* 2015;27(2):481-483.
24. Busscher I, Ploegmakers JJ, Verkerke GJ, Veldhuizen AG. Comparative anatomical dimensions of the complete human and porcine spine. *Eur Spine J.* Jul 2010;19(7):1104-1114.

25. Jiang H, Moreau M, Raso VJ, Russell G, Bagnall K. A comparison of spinal ligaments-- differences between bipeds and quadrupeds. *J Anat.* 1995;187(Pt 1):85-91.
26. Kim AJ, University of California SFwtUoC, Berkeley. Bioengineering. *In Situ Regeneration of the Nucleus Pulposus*: University of California, San Francisco with the University of California, Berkeley; 2009.
27. Chan SC, Lam S, Leung VY, Chan D, Luk KD, Cheung KM. Minimizing cryopreservation-induced loss of disc cell activity for storage of whole intervertebral discs. *Eur Cell Mater.* Jun 09 2010;19:273-283.
28. Armitage WJ. Cryopreservation of animal cells. *Symp Soc Exp Biol.* 1987;41:379-393.

**FIGURE LEGENDS**

**Figure 1.** Schematic of the in vitro experiment setup. Each porcine intervertebral disc is sandwiched between 2 squares of screen under a perforated cylinder, and weights are placed in a smaller bucket set on top of them. The fluid poured into the bottom bucket reaches approximately halfway up the perforated cylinder. *Used with permission from Barrow Neurological Institute, Phoenix, Arizona.*

**Figure 2.** (A) Photograph showing the test fixture. (B) Photograph of test setup. *Used with permission from Barrow Neurological Institute, Phoenix, Arizona.*

**Figure 3.** Photographs of stained intervertebral discs cut in half. (A-D) The discs were stained with Safranin O for (A) 1 day, (B) 3 days, (C) 5 days, and (D) 7 days in the diffusion-only model. *Used with permission from Barrow Neurological Institute, Phoenix, Arizona.*

**Figure 4.** The calculated depth of stain penetration into the annulus fibrosus for the Safranin O diffusion only sample (solid black line), the Fast Green FCF diffusion only sample (solid gray line), and the Safranin O compressed sample (dashed black line). Time points with the same number of asterisks (\* or \*\* or \*\*\*) indicate a significant difference between those time points as determined by the *t* test ( $P < 0.02$ ). *Used with permission from Barrow Neurological Institute, Phoenix, Arizona.*

**Figure 5.** The nucleus pulposus staining score (1= none, 2= partial, and 3= full) for the Safranin O (SO) diffusion (black bars), Fast Green FCF diffusion samples (white bars), and SO compressed (gray crosshatched bars). Asterisks (\*) indicate significance between time points as determined by the Mann-Whitney U test ( $P = 0.004$ ). Error bars indicate standard deviation. *Used with permission from Barrow Neurological Institute, Phoenix, Arizona.*

**Figure 6.** (A) The nucleus pulposus staining score and (B) the depth of annulus fibrosus that was stained in compressed samples with open end plates ( $P=0.07$ ) and with blocked end plates ( $P=0.25$ ). Error bars indicate standard deviation. *Used with permission from Barrow Neurological Institute, Phoenix, Arizona.*

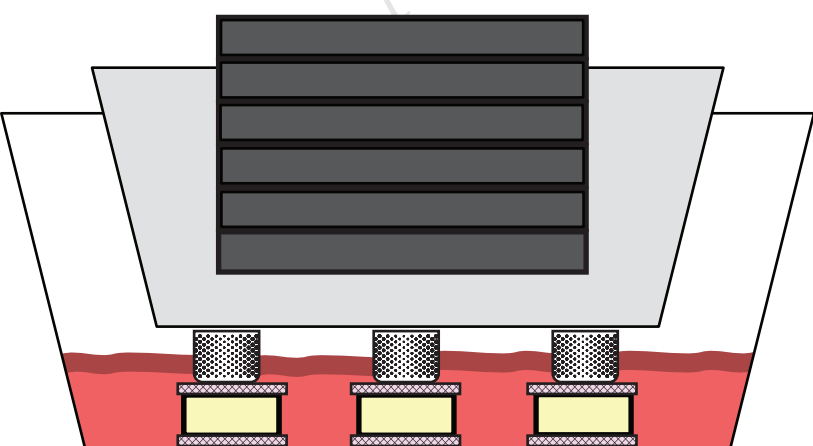
**Figure 7.** (A) The nucleus pulposus staining score with Safranin O ( $P=0.07$ , Kruskal-Wallis) and (B) the depth of annulus fibrosus that was stained with Safranin O ( $*P=0.04$ ,  $t$  test) in samples under traction, compression, or diffusion only (no load). Asterisks indicate a significant difference between loading groups. Error bars indicate standard deviation. *Used with permission from Barrow Neurological Institute, Phoenix, Arizona.*

**Table 1.** Literature review of nutrient transport in the intervertebral disk.

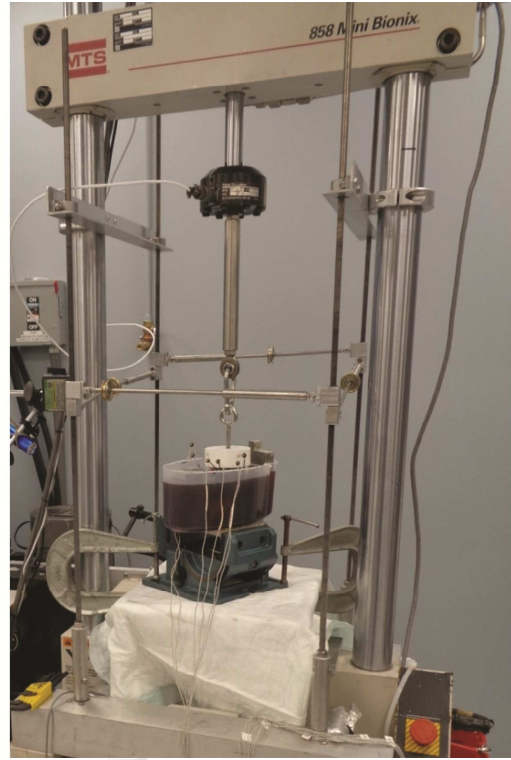
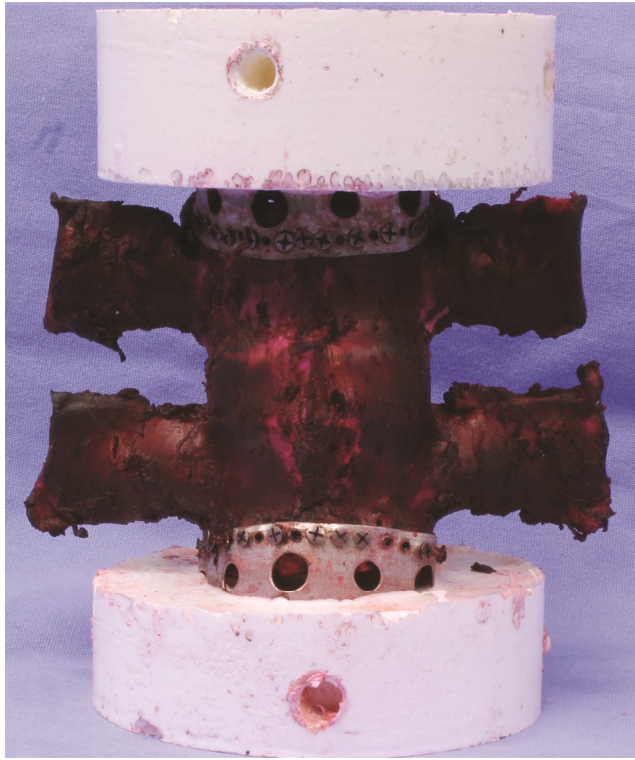
Reference	Publication Year	Key Findings of Study		Method
		Compression	Convection	
Urban et al. <sup>15</sup>	1982	No effect		Canine in vivo radioactive tracer injection
Ferguson, Ito, & Nolte <sup>16</sup>	2004		Increases transport of large molecules; no effect on small molecules	Mathematical model
Soukane et al. <sup>17</sup>	2007	Increases transport		Mathematical model
Huang and Gu <sup>18</sup>	2008	Decreases transport		Mathematical model
Arun et al. <sup>19</sup>	2009	Decreases transport		Human in vivo contrast-enhanced MRI
Jackson et al. <sup>8</sup>	2011	Decreases transport		Mathematical model
Malandrino et al. <sup>7</sup>	2011	Increases transport	No effect	Mathematical model
Zhu et al. <sup>20</sup>	2012		Increases transport	Mathematical model
Gullbrand et al. <sup>10</sup>	2015	Increases or decreases transport, depending on load		Rabbit in vivo contrast-enhanced MRI

Abbreviation: MRI, magnetic resonance imaging.





- |                                                                                                 |                                                                                                         |
|-------------------------------------------------------------------------------------------------|---------------------------------------------------------------------------------------------------------|
|  Screen       |  Disc                |
|  Weight Plate |  Perforated Cylinder |



ACCEPTED MANUSCRIPT

